

doi:10.7515/JEE201604005

伊犁尼勒克黄土石英颗粒微形态特征及其成因与物源意义

李 越¹, 宋友桂¹, 赵井东²

(1. 中国科学院地球环境研究所 黄土与第四纪地质国家重点实验室, 西安 710061;
2. 中国科学院寒区旱区环境与工程研究所, 兰州 730000)

摘要: 石英颗粒表面微形态分析是判断沉积物成因和来源的重要方法之一。对伊犁盆地尼勒克黄土石英颗粒表面微形态特征进行了研究, 并将其与冰川、河流、沙漠样品进行比较, 结果表明尼勒克黄土石英颗粒磨圆较差, 冰川和水流作用的微形态特征明显, 系近源风力搬运沉积。通过对比分析讨论了石英粉砂的可能产生机制, 认为流水和寒冻风化作用为伊犁黄土的形成提供了重要动力来源。尼勒克黄土的物质来源和匈牙利黄土类似, 而与黄土高原黄土有较大差别, 这主要表现在经受风力搬运-沉积的次数上或者风力搬运的距离上。该研究为解译伊犁地区黄土的古气候环境意义提供了重要基础。

关键词: 伊犁黄土; 石英颗粒表面结构; 成因与来源

Micromorphological characters of quartz grain from Nilke loess-paleosol sequences and their implications of origin and provenance

LI Yue¹, SONG Yougui¹, ZHAO Jingdong²

(1. State Key Laboratory of Loess and Quaternary Geology, Institute of Earth Environment,
Chinese Academy of Sciences, Xi'an 710061, China;
2. Cold and Arid Regions Environmental and Engineering Research Institute,
Chinese Academy of Sciences, Lanzhou 730000, China)

Abstract: *Background, aim, and scope* Xinjiang is also one of the most significant loess regions in China with the exception of Chinese Loess Plateau, and the loess is mainly present in the northern piedmont of the Tianshan and Kunlun Mountains and Ili Basin. The loess deposits in Ili Basin unconformably cover the river terraces, the low uplands and the slopes of the Tianshan Mountains, and the researches on them have the merit of enabling reconstructions of past climate change in westerly dominant area of inland Asia. Although many predecessors have investigated the spatial distribution and studied the ages, pedostratigraphy, rock magnetism, elemental and mineral compositions and their implications for paleoclimate in details with respect to the Ili loess, there are many urgent questions that need to be solved: How were the materials

收稿日期: 2016-03-10; 录用日期: 2016-06-13

Received Date: 2016-03-10; **Accepted Date:** 2016-06-13

基金项目: 国家自然科学基金项目(41572162, 41172166); 中国科学院地球环境研究所自主部署重点项目(ZZBS1301); 中国科学院科技创新“交叉与合作团队”项目(中科院人字[2013]47号); 中国科学院国际合作局对外合作重点项目(132B61KYS20160002)

Foundation Item: National Natural Science Foundation of China (41572162, 41172166); Key Research Program of Institute of Earth Environment, Chinese Academy of Sciences (ZZBS1301); Cross-disciplinary Collaborative Teams Program for Science, Technology and Innovation of Chinese Academy of Sciences (Renzi [2013]47); International Partnership Program of Chinese Academy of Sciences (132B61KYS20160002)

通信作者: 宋友桂, E-mail: ygsong@loess.llqg.ac.cn

Corresponding Author: SONG Yougui, E-mail: ygsong@loess.llqg.ac.cn

of Ili loess generated? Which geological process was experienced by the loess silt particles before they reached the sediment area? And where is the provenance of Ili loess? We have had no understanding of the answers by far, which hampers the interpretation of climate change. For this reason, this paper aims to solve the problems above mentioned with the micromorphological characters of quartz grains. In recent study, we compared the micromorphology of quartz grains from Nilka loess with those from glacial tills, riverbed deposits and desert sands to determine the mechanisms of loess-sized quartz silt production. These works will lay the foundation for the subsequent studies on the Ili loess. **Materials and methods** The 4 loess samples were collected from Nilka section located at the second-order terrace of Kashi River in the east of Ili Basin with the depths 1.50 m, 9.10 m, 11.06 m and 19.56 m, respectively. Glacial till was sampled from the terminus of Arqialeter Glacier located in catchment area of Xiate River; riverbed deposits were sampled from Kashi River and the sampling sites lay in the west of Nilka loess section; desert sands were sampled from Kyzylkum, Muyunkum and Saryesik Atyrau desert within Kazakhstan respectively. With regard to the loess, 2 g dried sample was weighed, then hydrogen peroxide and hydrochloric acid were added to remove the organic matters and carbonates, and finally the quartz minerals were separated by hydrofluosilicic acid (H_2SiF_6) treatment. We chose the quartz grains within the grain sizes of 20—70 μm for observation. For glacial till, riverbed deposits and desert sands, first, organic matters and carbonates were removed from these samples with the same method; second, remnant materials were dried and sieved through 0.125 mm; third, quartz grains of <0.125 mm were selected under binocular microscope. All the quartz grains were mounted on the SEM (scanning electron microscope) stubs with conductive tapes and sputtered with gold, and morphologic observation were conducted with PhenomTM proX (energy spectrum version) at the Environmental Mineralogy Laboratory, State Key Laboratory of Loess and Quaternary Geology. After that, frequency of each texture's occurrence was calculated. **Results** The results reveal that the quartz grains from Nilka loess are poorly rounded; microtextures produced by glaciation and fluviation are obvious but those by aeolian abrasion are rare; the chemical dissolution developed well in the surface of quartz grains but very few chemical precipitation could be observed. **Discussion** In spite of the surface with sharp feature, we are quite confident that Nilka loess is the eolian sediment according to previous literatures and the grain size distribution characteristics. With the Euclidean distances, we found that the loess was nearest to riverbed deposit and farther away from glacial till, and had farthest distance to desert sand. This result suggested the significant impact of flow action on the generation of loess quartz silt and a certain contribution from glaciation. By analyzing the characteristics of tectonic environment in Tianshan region, combined with silt generating mechanisms reported by predecessors, we also considered the freezing weathering in high elevation area as one of the silt generating mechanisms. With comparative analysis to probable sequence of events indicating the formation of loess, it holds that the origin of Nilka loess are similar to those of loess in Hungary but different from those of loess in Chinese Loess Plateau. **Conclusions** With the studies of surface micromorphological characters of quartz grain and the grain size, we believe that Nilka loess also belongs to eolian sediment, and the shape of particle and morphology by mechanical effect indicate that Nilka loess materials have experienced glaciation and flow action before transportation by wind. The flow action played an important role in the generation of quartz silt from Nilka loess and glacial abrasion might make a certain contribution. However eolian erosion leaved no obvious traces in surface of quartz particles, indicative of the shorter transporting distance by wind between loess deposit area and provenance. Moreover it is inferred that the weather denudation was also the important silt generating mechanism. The origin of Nilka loess are similar to those of loess in Hungary, but different from those of loess in Chinese Loess Plateau, which displays mainly in the time of transportation-deposition by wind or distance of wind transport. **Recommendations and perspectives** This paper analyzes the geologic processes experienced by

Nilka loess materials and gives a understanding of the loess silt generating mechanism with plotting the probable sequence of events indicating the formation of loess. This work will lay an important foundation for interpreting climatic significance of Ili loess.

Key words: Ili loess; quartz grain textures; origin and source

在我国，黄土除了在黄土高原集中分布外，位于亚洲内陆的新疆地区也有广泛的黄土堆积，如伊犁盆地、天山和西昆仑山坡麓。伊犁盆地的黄土主要分布在低山、丘陵和高阶地上（叶玮等，2003）。近十多年来，众多学者（史正涛等，2007；宋友桂等，2010a, 2010b；李传想等，2011, 2012；李传想和宋友桂，2011, 2014；Zhang et al., 2013；鄂崇毅等，2014；曾蒙秀和宋友桂，2014；Song et al., 2014；Yang et al., 2014）对新疆伊犁黄土的分布特征、年代、粉尘来源、化学风化特征、粒度、磁学和矿物学等方面的特征进行了分析，进一步探讨了黄土蕴含的古气候环境意义。然而黄土高原常用的磁化率和粒度指标在伊犁黄土中的古环境意义仍存在争论（叶玮，2001；史正涛等，2007；Song et al., 2008；李志忠等，2010；宋友桂等，2010a；夏敦胜等，2010；贾佳等，2011, 2012）。同时伊犁黄土物质如何产生？黄土粉尘在到达沉积区前经历了哪些地质作用？是风成为主，还是近距离搬运？黄土的物源又在哪里？到目前为止，这些问题都没有得到很好解决，妨碍了伊犁黄土的古气候指标的解译。为解决以上问题，本文利用石英颗粒表面特征来研究黄土成因与来源问题。

由于石英在地表环境下具有稳定的物理和化学特性，因此其颗粒形态特征可以用来反映沉积物的源区、搬运动力和沉积后的改造（刘东生，1985；Pye, 1987；Guo et al., 2002）。不同环境下的石英颗粒表面具有不同的形态及其组合特征（谢又予，1984；Krinsley and Trusty, 1985；Vos et al., 2014），因此可以利用这些特征对沉积物成因进行直观判别（Krinsley and Donahue, 1968；Helland et al., 1997；李珍等，1999；Newsome and Ladd, 1999）。通过对伊犁盆地尼勒克黄土的石英颗粒形态和表面微结构的研究，并将其形态特征组合同来自冰川、河流和沙漠的样品进行对比，来探讨该地区黄土中石英粉砂的产生机制，分析黄土物质的形成过程及其与黄土高原黄土、欧洲黄土的异同。

1 样品的采集、制备与分析方法

1.1 样品的采集

为了确定伊犁盆地黄土形成过程与所经历过的沉积环境，采集了伊犁盆地东部黄土、现代沙漠、河流沉积物、冰碛物的样品（图1），进行了石英颗粒表面微形态的研究。沙漠样品来自伊犁盆地西边哈萨克斯坦的克孜勒库姆沙漠、木尤思沙漠和萨雷耶西克阿特劳沙漠沙，样品号分别是KZ45、KZ60和KZ84（图1a）。冰川样品采自天山夏特河流域阿尔恰勒特尔冰川末端冰碛物（图1b），样品编号GL-XT；河床砂样品来自尼勒克剖面以西的喀什河（图1b），样品编号为YL1420、YL1421和YL1423；尼勒克剖面（图1c）位于伊犁盆地东部喀什河河流二级阶地上（图1b），剖面地理位置为 $83^{\circ}15'0.5''E$ 、 $43^{\circ}46'6''N$ ，海拔高度为1558 m，剖面厚20.5 m，主要由2层砂黄土和2层弱古土壤组成，底部砂砾石层出露（Song et al., 2015）。为避免成壤作用造成的化学溶蚀和沉淀对石英颗粒原始表面特征的影响，本文仅使用来自黄土层的样品，取样深度分别是1.50 m、9.10 m、11.06 m和19.56 m。

1.2 样品制备

黄土样品中石英的分离采用改进了的焦硫酸钾-氟硅酸浸泡法（Xiao et al., 1995；孙有斌，2001），即取风干样品2 g，加双氧水和盐酸除去有机质、碳酸盐和铁氧化物，然后用焦硫酸钾熔融-氟硅酸浸泡法提取样品中的单矿物石英。此方法得到的石英表面干净，纯度可达95%以上（图2）。而对于冰川、河流与沙漠样品，处理步骤如下：称取10 g样品，加入30%的H₂O₂溶液静置48 h后，加热煮沸以除去有机物。然后将样品置于浓度为15%的盐酸中，煮沸15 min，去除石英砂颗粒表面黏附的碳酸盐类矿物。用蒸馏水反复冲洗后烘干。颗粒表面形态特征与粒度有关（Porter, 1962；Mahaney, 2002），尤其对于沙漠石英砂，其颗粒越粗，磨圆度增加（夏训诚，1987）。研究认为0.125—0.01 mm石英砂除少数颗粒为硅质

覆盖外, 完全可以反映成因类型, 表面结构成因组合发育较全(方小敏, 1991), 所以将烘干的样品过0.125 mm筛, 使测试的颗粒粒径与尼勒克黄土石英粒径相接近, 以减少由于粒径差异带来的误差。然后在40倍双目显微镜下从每个河流和沙漠样品中分别挑选出石英颗粒40粒以上; 在冰川样品中挑选出48粒石英颗粒。根据Pye(1987)的研究, 20—70 μm的粒级为短距离的悬移组分, 并且其为尼勒克黄土粒度的主要组分, 因此本文

主要观测黄土中该粒级组分的石英颗粒来提取环境信息和物质来源信息。每个黄土样品测试100粒左右。将样品用导电碳胶带固定并镀金后, 置于飞纳台式扫描电镜PhenomTM proX(能谱版)下观察。在对挑选的石英颗粒进行拍照之前, 先用电镜自带的能谱仪(EDS)确定为石英颗粒, 然后进行表面形态特征统计分析。以上实验过程在黄土与第四纪地质国家重点实验室环境矿物学实验室完成。

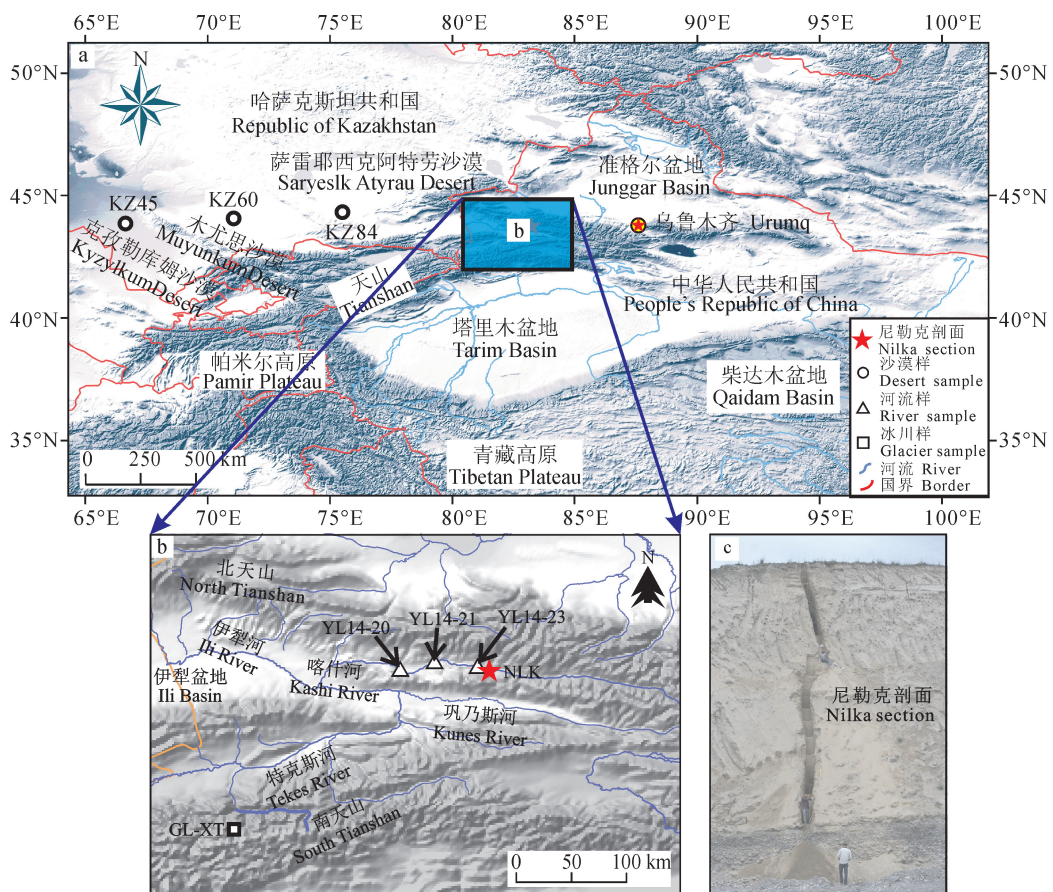


图1 采样点分布图(a, b)和尼勒克黄土剖面(c)
Fig.1 Location of the samples (a, b) and the Nilka loess section (c)

1.3 统计分析方法

利用石英颗粒表面特征来判断物质的来源或成因时, 一般要用特征组合来进行分析。本文综合前人(谢又予, 1984; 王颖和迪纳瑞尔, 1985; 潘仁义等, 2012)对石英颗粒表面特征的划分方案进行划分, 分析方法采用环境颗粒百分比法(含有某种特征的颗粒占全部被分析颗粒的百分比)(陈丽华等, 1986)。

2 结果与讨论

2.1 石英颗粒形态总体特征

尼勒克黄土石英颗粒以多棱角状、多边形状和次棱角状为主, 次圆状颗粒极少出现或不出现, 未见圆状颗粒(图3)。边缘形状多表现为棱脊磨损和尖棱脊, 次棱脊出现频率平均为14%左右, 有少量亚圆边缘出现, 但频率略大于2% (图4a), 未见磨圆边缘。

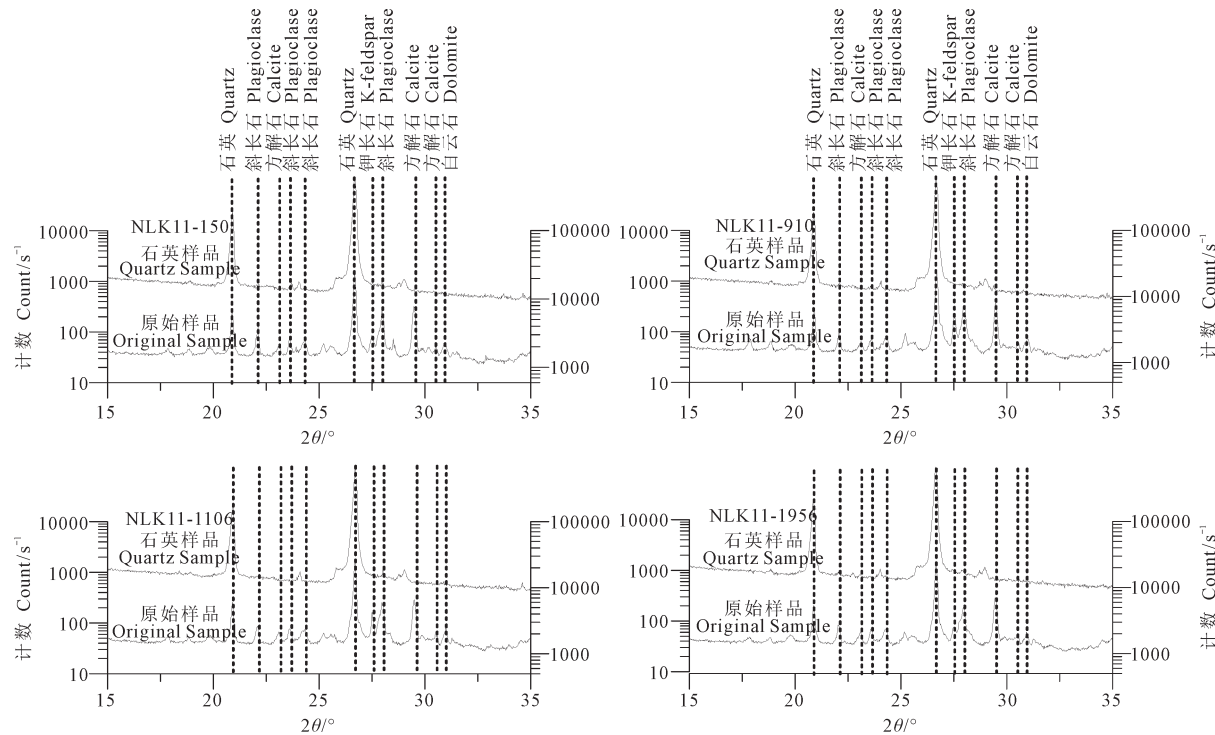


图2 石英样和原样X射线衍射图谱对比

Fig.2 Comparison of X-Ray diffraction spectrums between extracted quartz and bulk samples in NLK section

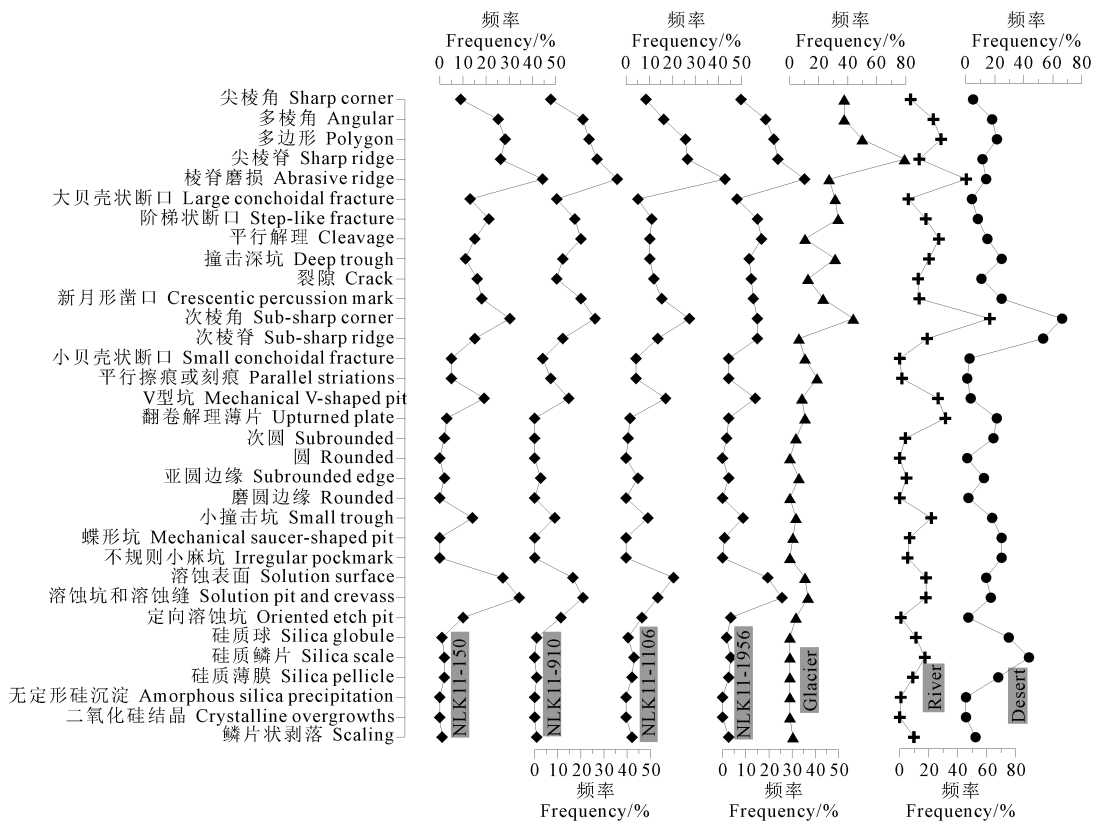
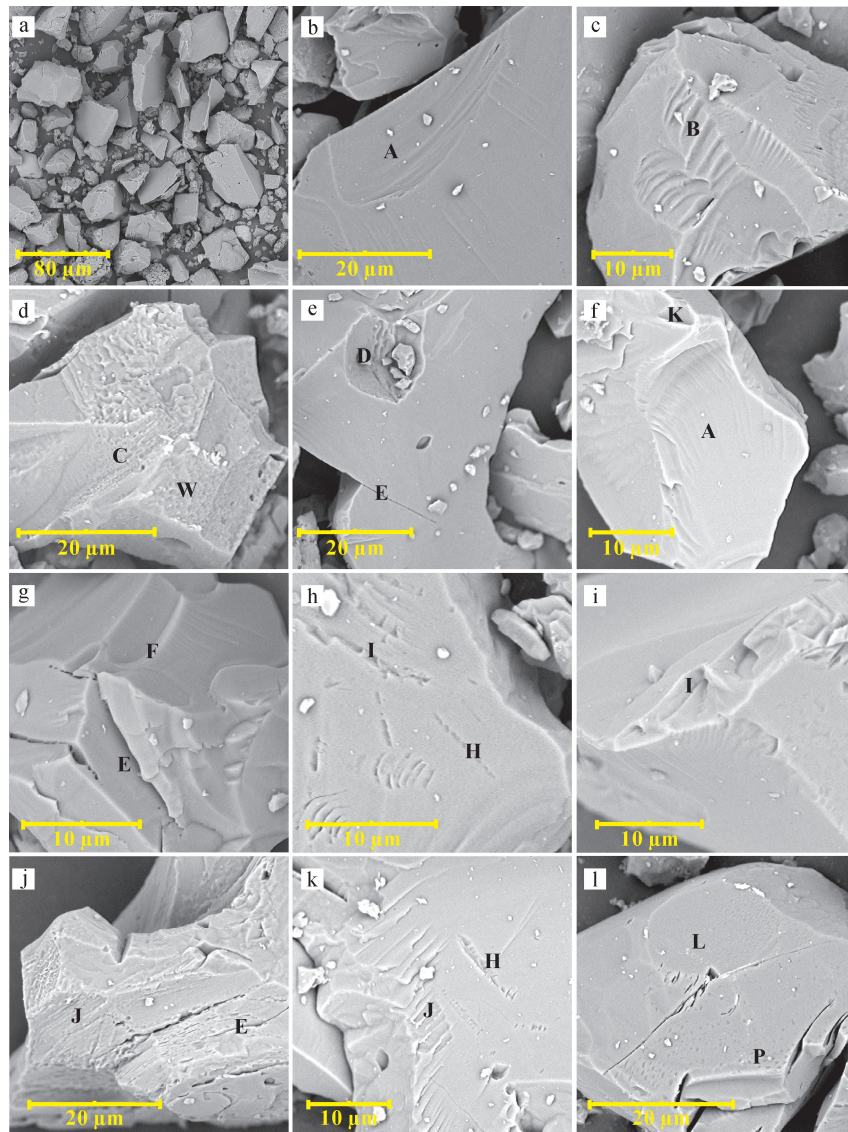


图3 尼勒克剖面黄土与不同环境沉积物石英颗粒表面形态特征曲线对比（冰川、河流和沙漠曲线是样品的平均值）

Fig.3 The curve of quartz surface texture in NLK section and comparison of those from different environments



A: 大贝壳状断口; B: 阶梯状断口; C: 平行解理; D: 撞击深坑; E: 裂隙(纹); F: 新月形凿口; H: 平行擦痕或刻痕; I: V型坑; J: 翻卷解理薄片; K: 小撞击坑; L: 蝶形坑; N: 溶蚀表面; O: 溶蚀坑和溶蚀缝; P: 定向溶蚀坑; W: 鳞片状剥落
 A: Large conchoidal fracture; B: Step-like fracture; C: Cleavage; D: Deep trough; E: Crack; F: Crescentic percussion mark; H: Parallel striations; I: Mechanical V-shaped pit; J: Upturned plate; K: Small trough; L: Mechanical saucer-shaped pit; N: Solution surface; O: Solution pit and crevass; P: Oriented etch pit

图4 尼勒克黄土石英颗粒SEM外形特征(a)与机械作用结构特征(b—l)(含部分化学作用结构形态)
 Fig.4 Surface microtopography (a) and mechanical microtextures (b—l) (Including part of chemical microtextures) of quartz grains under scanning electron microscope

2.2 机械作用形态

2.2.1 贝壳状断口与阶梯状断口

一般认为石英颗粒的贝壳状断口在冰川环境中大量产生 (Vos et al., 2014)。而在风力长距离的搬运过程中, 贝壳状断口往往会被磨蚀或改造而消失, 因此在沙漠环境中少见。在高能水成环境中由于水的缓冲作用, 颗粒产生的贝壳状断口

少且面积较小, 而中低能水下环境则不会产生 (谢又予, 1984; 陈丽华等, 1986)。尼勒克黄土石英颗粒表面贝壳状断口多呈清晰的弧形, 其上发育新鲜的解理片, 且出现相互重叠的现象 (图 4b, 4f)。黄土石英颗粒中大贝壳状断口 ($>10 \mu\text{m}$) 出现频率为 5%—13%, 平均为 9%, 而小贝壳状断口出现频率较小, 变化于 3%—5%, 平均为 4%

(图 3)。因此, 黄土物质经历过冰川作用后, 受到了后期河流流水的作用。

阶梯状断口往往出现在贝壳状断口与解理面相交处, 呈现弧状或平直状, 其形成与挤压作用或猛烈撞击作用有关, 冰川作用、泥石流、洪流作用都可以形成。尼勒克黄土石英颗粒表面阶梯状断口出现频率为 11%—21%, 平均为 16% (图 3、图 4c, 4j 和图 5t), 这也说明黄土石英颗粒在某一段时间内受到过较大的机械应力作用。

2.2.2 平行解理

平行解理常常与贝壳状断口或平直状断口 (阶梯状断口) 一起出现, 其形成同样也与颗粒的碰撞或挤压有关。尼勒克黄土平行解理出现频率为 10%—20%, 平均为 16% (图 3 和图 4d), 进一步证实黄土石英颗粒在搬运过程中遭受过较强的外力碰撞作用。

2.2.3 撞击深坑与 V 型坑

石英颗粒在搬运过程中, 受到强烈的撞击从而造成深坑。尼勒克黄土撞击深坑出现频率平均为 11%。V 型坑同样是机械撞击、磨损而留下的痕迹, 其几乎全部在高能的水下环境中通过颗粒相互碰撞形成 (Mahaney and Kalm, 2000), 代表高能机械环境, 可以作为水下磨蚀作用的标志特征 (陈丽华等, 1986)。尼勒克黄土石英颗粒 V 型坑出现的频率为 14%—19%, 平均为 16% (图 3 和图 4e, 4h, 4i), 由此可见, 该地黄土在搬运过程中经常受水流作用的影响。

2.2.4 平行擦痕或刻痕

平行擦痕或刻痕是在较高压力下, 棱角尖锐的颗粒之间相对挤擦发生位移时产生的 (Krinsley and Donahue, 1968), 可以作为冰川环境的诊断性特征 (Higgs, 1979)。尼勒克黄土擦痕或刻痕出现的频率较小, 为 2%—5%, 平均为 3% (图 3 和图 4h, 4k, 4l)。从此结果来看, 似乎冰川磨蚀对尼勒克黄土物质的产生影响较小。

2.2.5 新月形凿口

石英颗粒在高压下经过大颗粒的缓慢研磨形成新月形凿口, 其弧形顶端指示的方向与最大刻蚀应力平行。在尼勒克黄土石英颗粒中的出现频率为 13%—20%, 平均为 17% (图 3、图 4g 和图 5o)。潘仁义等 (2012) 发现新月形凿口在天山冰川沉积石英砂颗粒出现的频率较高, 然而石磊等 (2009) 发现新月形凿口在贡嘎山海螺

沟冰碛物极少出现。两者分析的石英砂颗粒的粒度相同。因此笔者认为新月形凿口对冰川作用的指示还存在不确定性, 本文暂不对其进行讨论。

2.2.6 翻卷解理薄片

翻卷解理薄片是一系列呈锯齿状, 高度参差不齐的薄的平行解理片, 与颗粒表面之间存在一定的夹角 (Margolis and Krinsley, 1974)。翻卷解理薄片一般都经受了溶蚀和沉淀作用, 尤其是在热带沙漠地区 (陈丽华等, 1986; Mahaney, 2002)。它是风成和冰川环境的主要特征 (Krinsley and Cavallero, 1970; Mahaney, 2002; Costa et al, 2013), 但是一般在风成环境中比较普遍。其在黄土石英中极少出现 (2%) (图 3、图 4j 和图 5m), 也表明该地黄土只经历过较短距离或时间的风力搬运。

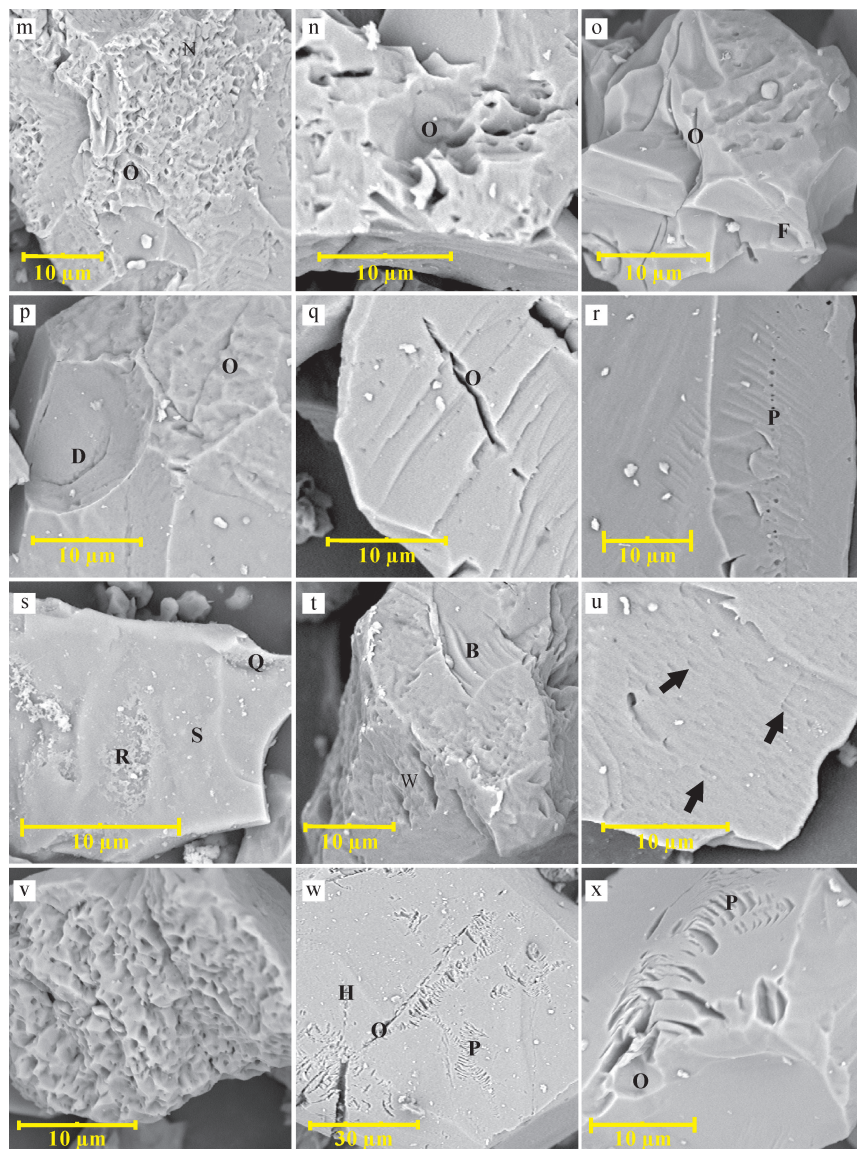
2.3 化学作用形态

2.3.1 溶蚀作用

由于本文未使用古土壤样品, 因此可以认为石英颗粒上的溶蚀痕迹均产生于被风力搬运至沉积区前。尼勒克黄土石英颗粒中溶蚀表面、溶蚀坑和溶蚀缝的出现频率较高, 分别为 21%、26% (图 3、图 4d, 4l 和图 5 m—q)。不规则溶蚀坑的出现说明化学作用已经深入到解体带与非解体带之间的过渡带; 石英 r 面 ($10\bar{1}1$) 晶面缺陷形成的蚀坑 (图 5u 中黑色箭头处) 多次出现; 有的颗粒表面化学溶蚀强烈发育, 形成了蜂窝状溶蚀坑 (图 5v)。

定向溶蚀坑有一定方向性 (图 4b, 4l 和图 5q, 5r), 其产生与晶体晶格错位和缺陷有关 (Amelinckx, 1964)。它们有的外表很像等腰三角形, 并且成排出现 (图 5x), 有时见到两排交叉在一起, 呈 X 结 (图 5w)。这种溶蚀坑先后经历了机械和化学两类作用 (Bull et al, 1980; Bull, 1981; Peterknecht and Tietz, 2011)。它们在冰川环境下普遍存在, 而在其他环境中鲜见报道 (Vos et al, 2014)。其出现频率不及 10% (图 3), 可能反映了颗粒处于冰川环境的时间较短。

鳞片状剥落与晶体缺陷、杂质以及撞击形成的裂缝有关, 其出现仅限于发生溶解淋滤的成壤层位 (Higgs, 1979)。而在黄土石英颗粒中极少出现 (2%) (图 3、图 4d 和图 5t), 表明该地黄土的成壤作用很弱。



B: 阶梯状断口; N: 溶蚀表面; D: 撞击深坑; F: 新月形凿口; H: 平行擦痕或刻痕;
J: 翻卷解理薄片; O: 溶蚀坑和溶蚀缝; P: 定向溶蚀坑; S: 硅质薄膜; R: 硅质鳞片;
Q: 硅质球; W: 鳞片状剥落
B: Step-like fracture; N: Solution surface; D: Deep trough; F: Crescentic percussion mark;
H: Parallel striations; J: Upturned plate; O: Solution pit and crevass; P: Oriented etch pit;
S: Silica pellicle; R: Silica scale; Q: Silica globule; W: Scaling

图 5 尼勒克黄土石英颗粒 SEM 化学作用结构特征 (m—x) (含部分机械作用结构形态)
Fig.5 Chemical microtextures (m—x) of quartz grains under SEM (scanning electron microscope)
(Including part of mechanical microtextures)

2.3.2 沉淀作用

硅质球、硅质鳞片和硅质薄膜是常见的氧化硅沉淀形式, 沉淀作用程度逐渐加大, 图 5s 记录了从硅质球到硅质薄膜的演化。但是黄土石英颗粒表面这类沉淀作用极少出现(图 3)。

一般认为石英晶体的增长反映的是次生变化特征, 而不是沉积环境特征(江新胜等,

2003a, 2003b), 它的形成与埋深、在过饱和溶液中的滞留时间以及可用空间有关(Pittman, 1972; Marzolf, 1976)。石英晶体的增长需要较长的时间(Higgs, 1979), 而尼勒克黄土石英颗粒表面未见无定形硅沉淀以及二氧化硅结晶, 说明石英粉砂颗粒未在某一地点停留太长时间。

2.4 黄土物质的形成

2.4.1 黄土的风成成因

在对尼勒克黄土石英颗粒形态进行观察时，发现其表面多见尖锐的棱角，贝壳状断口与阶梯状断口常见，而几乎未见蝶形坑与不规则的小麻坑，这似乎与黄土的风成成因相悖。但是这些特征与黄土高原西峰红粘土、甘肃秦安红粘土以及匈牙利 Tengelic 红粘土等典型的风成沉积物相似 (Guo et al, 2001; Liu et al, 2006; Kovacs et al, 2008)，都被看作是风成粉尘沉积物所具有的特征 (Whalley et al, 1982; Pye and Sperling, 1983; Pye, 1995; Wright, 2001)。粉尘颗粒在被搬运过程中处于悬浮状态，它们锐利的边缘未遭受到磨损，而这正好可以将黄土物质在被风搬运之前所经历的地质营力保留下来，便于了解黄土物质的产生过程。

尼勒克黄土风成成因另外的证据来自对其粒度的分析。黄土粒级在 10—50 μm 的颗粒含量为 47%—62%，占粒级组成的主要部分，其余粒组所

占比例较小（数据未发表）。而 Moldvay (1962) 的实验结果表明该粒级颗粒易浮动、易分散，称为风尘的“基本粒组”，由此推断尼勒克黄土亦为风成堆积。

2.4.2 黄土物质的动力来源

使用欧几里得直线距离计算方法 (Mahaney et al, 2001)，将黄土石英颗粒表面特征组合同冰川、河流与沙漠石英样品进行比较。该方法基于石英颗粒表面微形态特征百分比可定量反映两种沉积物形成环境的相似性。其计算公式如下：

$$d_{ij} = \sqrt{\sum_{k=1}^p (x_{ik} - x_{jk})^2} \quad (1)$$

其中： d 表示两种沉积物形成环境 i 与 j 之间的距离，其范围为 0 到 $+\infty$ ； p 表示统计的微形态特征的个数； x 表示某个微形态特征出现的频率。

计算结果如表 1 所示，冰川与沙漠、河流之间的距离都较远，沙漠与河流之间的距离相对较为接近。黄土同河流最近，其次是冰川，而离沙漠最远。

表 1 不同沉积物石英颗粒表面形态出现频率的欧几里得距离
Tab.1 Euclidean distances between frequencies of quartz grain surface textures

	黄土	Loess	冰川	Glacier	河流	River	沙漠	Desert
黄土	Loess	0						
冰川	Glacier		85.4	0				
河流	River		60.53	101.49	0			
沙漠	Desert		99.23	128.87	74.68	0		

该结果显示尼勒克黄土石英粉砂曾受到较长时间的水流作用。同时水流作用还是一种产生粉砂级物质的有效机制 (Wright et al, 1998)，短距离的河流搬运就可以使得较小的颗粒进一步遭受粉碎 (Schumm and Stevens, 1973)。黄土石英颗粒表面上 V 型坑的出现频率相对较高 (图 3)，也说明水流作用对黄土粉砂物质的产生起到了重要的影响 (Pye, 1995; Gallet et al, 1998; Wright, 2001; Smalley et al, 2009)。另外在河流样品中，阶梯状断口与平行解理的出现频率高于冰川与沙漠样品 (分别为 18%、27%)，表明产生这两种微形态的机械应力主要来自于水体的流动。因此可以推断尼勒克黄土石英颗粒表面阶梯状断口与平行解理的出现频率较高 (都为 16%)，其原因主要是受到水流的作用。

Smalley (1990) 认为在中亚的高山地区，第

四纪冰川活动十分有限，则大量粉砂级物质的产生应与除冰川作用之外的其他机制有关。这从本文所统计的擦痕或刻痕出现的频率上也能看出 (图 3)。Wright et al (1998) 虽然通过模拟实验也证明了冰川磨蚀并不是石英粉砂产生的非常有效的机制，但是其仍然认为在自然环境下冰川磨蚀可长期持续地产生粉砂物质。由此，本文认为冰川磨蚀在粉砂物质产生方面具有一定作用，但是冰川与黄土的石英颗粒形态特征之间的欧几里得距离不及河流，一方面可能是因为冰川磨蚀确实无法供给大量的粉砂级物质；另一方面可能是冰川作用留下的痕迹受到后期流水作用的改造。

尽管冰川作用对粉砂物质产生的影响较小，但是高海拔地区的风化作用是非常有效的石英粉砂产生机制，这由前人的实验也得到证明 (Wright

et al, 1998), 因此本文认为高山地区的风化对尼勒克黄土物质的产生同样有重要的影响。新生代以来, 受印度板块向北俯冲碰撞的影响, 天山地区经历了强烈的隆升 (Avouac et al, 1993; 郭召杰等, 2006), 即使是在晚更新世晚期, 北天山仍然遭受了差异性抬升的过程 (杨晓平等, 2012)。因此, 伊犁黄土粉砂物质的产生与天山隆升带来的风化剥蚀加强也有密切关系: (1) 山体的隆升势必会造成由挤压、褶皱和俯冲所带来的构造应力的减小, 从而导致岩石的破碎和崩解; (2) 海拔的升高可以导致气候条件的改变, 增强寒冻风化; (3) 山体抬升还增加了流体的势能, 进而提高了冰川融水下切和沉积物剥蚀的速率。Smalley (1990, 1995) 也认为构造活动引发的风化作用对中国及中亚地区黄土的形成也是至关重要的。

黄土与沙漠样品的欧几里得距离最远, 也说明了粉砂颗粒在被搬运过程中处于悬浮状态, 未遭受到强烈的磨损。

另外, 尼勒克黄土石英表面的化学溶蚀现象十分发育 (图 3), 并且溶蚀作用基本发生在机械作用之后 (图 5), 也说明沉积物在经过短时间的冰川磨蚀、寒冻风化等作用之后即被融冰水搬运至冰水扇的扇缘地区。由于温度的升高, 沉积物经历了较强的化学溶蚀作用 (如潘仁义等 (2012) 对冰水沉积物石英颗粒表面形态的研究), 并且在搬运过程中可能也会产生一部分粉砂物质 (Nahon and Trompette, 1982; Pye, 1983)。化学沉淀作用在风成环境 (图 3) 和成岩作用中是普遍存在的 (陈丽华等, 1986), 而在尼勒克黄土石英颗粒上化学沉淀作用较少出现, 可能表明了该地黄土物质并没有长期处于类似沙漠的风成环境中。发源于中国天山的伊犁河干流由东向西流入哈萨克斯坦境内, 而伊犁盆地出现的大风、极大风又以西风、偏西风为主, 因此很可能石英粉砂在未被伊犁河水流搬运到盆地西部的沙漠时就已经被由西向东的气流吹扬起来。

综上所述, 天山岩体经受风化剥蚀、冰川磨蚀、冰水作用以及化学风化作用而产生的粉砂粒级物质被冰川融水或大气降水带到冰水冲积平原或冲积扇; 之后又被河流 (如伊犁河、喀什河) 搬运至盆地西部半干旱环境 (该环境条件更容易起尘 (Pye, 1995)) 下的河流冲积平原。另外可能也有一部分进入了干旱的沙漠环境; 最后这些沉积物又受到风力 (主要为近地面西风) 向东的搬运

作用, 而后堆积形成黄土。整个过程与 Smalley et al (2009) 的模型类似。其中在水流和风力的搬运过程中, 分选作用以及颗粒之间的碰撞也会对粉砂的聚集和产生有重要贡献 (Wright et al, 1998)。因此尼勒克地区黄土的形成过程可由图 6 来表示。

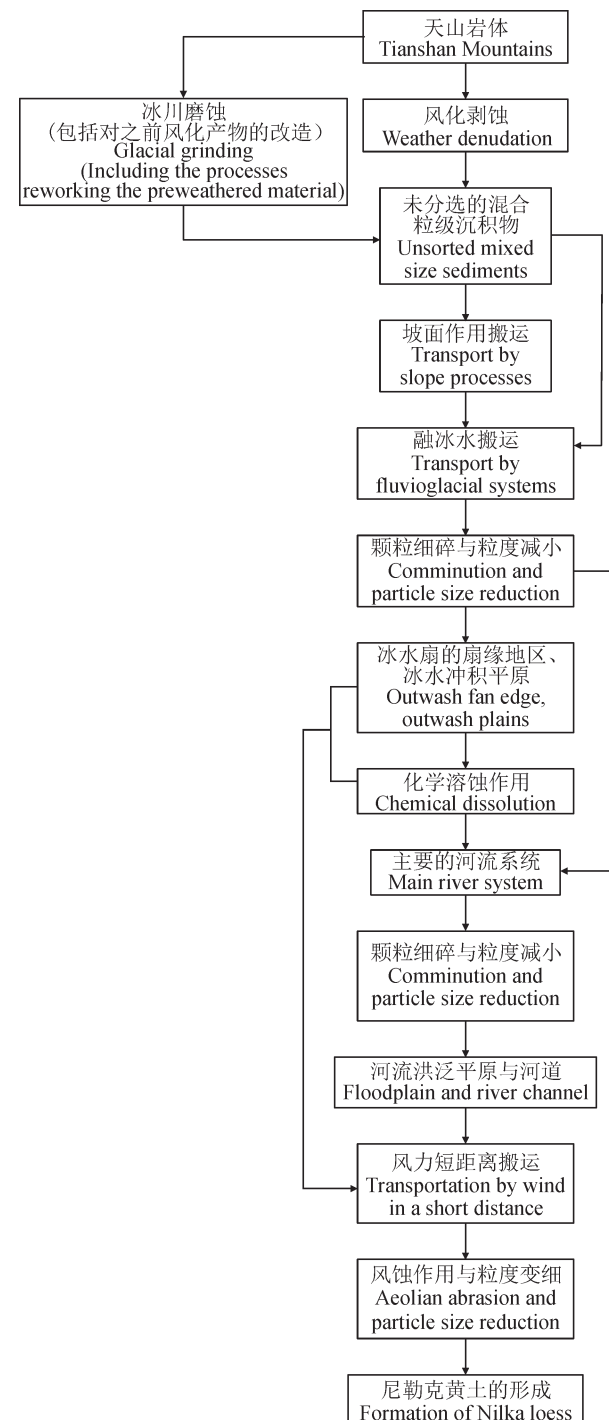


图 6 尼勒克黄土的形成过程
Fig.6 Probable mechanism of events the formation of Nilka loess

根据 Wright (2001) 的研究, 匈牙利黄土有如下形成过程: 喀尔巴阡山山体的风化、阿尔卑斯地区的寒冻风化以及北欧冰川分布区的冰川磨蚀产生大量的石英粉砂; 这些物质可以通过块体运动的形式或者冰川作用、坡面作用的方式向山下移动; 之后这些混合粒级的沉积物又被冰水、河流系统搬运而重新分配, 期间高能的水流系统也会造成颗粒的粉碎和粒级的变细。来自阿尔卑斯和喀尔巴阡山地区的沉积物分别由多瑙河和蒂萨河搬运至匈牙利大平原, 在泛滥平原沉积下来。最后经过风力侵蚀、搬运、沉积形成黄土; 而来自北欧更新世冰川作用区的物质经过冰水搬运到达冰水冲积平原后, 又经若干次河流搬运进入风力作用区, 之后在风力搬运、沉积后形成黄土。而黄土高原黄土与其西部或西北部的巨大山体之间存在有广阔的沙漠和戈壁, 冰川对阿尔泰山以及祁连山山体进行磨蚀以及寒冻风化所产生的粉砂物质首先要进入干旱的沙漠、戈壁等风成环境, 并且在该环境下经霜冻风化和盐风化还可以产生大量的粉尘, 因此黄土高原的黄土物质在到达沉积区前经历了多次风力搬运-沉积的过程。

从上面论述可以看出, 尼勒克黄土的形成与匈牙利黄土类似, 而同黄土高原黄土形成过程差异较大, 这主要表现在经受风力搬运-沉积的次数或者搬运的距离上。

3 结论

通过对尼勒克黄土石英颗粒表面形态特征的研究以及与冰川、河流、沙漠沉积物进行比较, 得到以下认识:

(1) 石英颗粒形态特征的研究, 结合粒度分析, 认为尼勒克黄土具有风成堆积的成因。石英颗粒外形以及机械作用形态特征指示尼勒克黄土物质在被风力搬运之前经受过冰川和水流的作用。

(2) 流水作用对尼勒克黄土石英粉砂具有重要的影响, 这不仅表现在石英粉砂的产生上, 而且还表现在水流可能对已有的粉砂级物质的改造上; 冰川磨蚀作用处于次要的位置; 而风力作用未在石英颗粒上留下明显的痕迹。山体隆升造成的风化剥蚀亦是黄土石英粉砂的重要产生机制。尼勒克黄土物质起源与匈牙利黄土类似, 在经受风力搬运-沉积的次数上或者风力搬运的距离上与黄土高原黄土有较大差异。

致谢: 本文在野外采样、实验操作以及论文写作当中得到了李云博士、陈涛硕士、周杰硕士、董俊超实验员以及北京大学刘耕年教授的帮助和指导, 在此表示衷心的感谢!

参考文献

- 陈丽华, 缪昕, 于众. 1986. 扫描电镜在地质上的应用 [M]. 北京: 科学出版社: 21-44. [Chen L H, Miao X, Yu Z. 1986. The applications of scanning electron microscope in geology [M]. Beijing: Science Press: 21-44.]
- 鄂崇毅, 杨太保, 赖忠平, 等. 2014. 中亚则克台黄土剖面记录的末次冰期以来的环境演变 [J]. 地球环境学报, 5(2): 163-172. [E C Y, Yang T B, Lai Z P, et al. 2014. The environmental change records since the Last Glaciation at Zeketai loess section, central Asia [J]. *Journal of Earth Environment*, 5(2): 163-172]
- 方小敏. 1991. 中国西部第四纪冰川与环境 [M]. 北京: 科学出版社: 138-148. [Fang X M. 1991. The quaternary glaciers in western China and the environment [M]. Beijing: Science Press: 138-148.]
- 郭召杰, 张志诚, 吴朝东, 等. 2006. 中、新生代天山隆升过程及其与准噶尔、阿尔泰山比较研究 [J]. 地质学报, 80(1): 1-15. [Guo Z J, Zhang Z C, Wu C D, et al. 2006. The Mesozoic and Cenozoic exhumation history of Tianshan and comparative studies to the Junggar and Altai Mountains [J]. *Acta Geological Sinica*, 80(1): 1-15.]
- 贾佳, 夏敦胜, 王博, 等. 2012. 黄土高原与伊犁黄土磁学特征对比及启示 [J]. 第四纪研究, 32(4): 749-760. [Jia J, Xia D S, Wang B, et al. 2012. The comparison between Loess Plateau and Ili loess magnetic properties and their implications [J]. *Quaternary Sciences*, 32(4): 749-760.]
- 贾佳, 夏敦胜, 魏海涛, 等. 2011. 阿西克剖面记录的西天山地区黄土磁学性质及古气候意义初探 [J]. 中国沙漠, 31(6): 1406-1415. [Jia J, Xia D S, Wei H T, et al. 2011. Magnetic property and paleoclimatic implication recorded by AXK sequence in West Tianshan area [J]. *Journal of Desert Research*, 31(6): 1406-1415.]
- 江新胜, 徐金沙, 潘忠习. 2003a. 鄂尔多斯盆地白垩纪沙漠石英砂颗粒表面特征 [J]. 沉积学报, 21(3): 416-422. [Jiang X S, Xu J S, Pan Z X. 2003a. Microscopic features on quartz sand grain surface in the Cretaceous desert of Ordos Basin [J]. *Acta Sedimentologica Sinica*, 21(3): 416-422.]

- 江新胜, 徐金沙, 潘忠习. 2003b. 四川盆地白垩纪沙漠石英砂颗粒表面特征 [J]. 沉积与特提斯地质, 23(1): 60–68. [Jiang X S, Xu J S, Pan Z X. 2003b. The surface features of the quartz sand grains from the Cretaceous desert in the Sichuan Basin [J]. *Sedimentary Geology and Tethyan Geology*, 23(1): 60–68.]
- 李传想, 宋友桂, 千琳勃, 等. 2011. 中亚昭苏黄土剖面粒度记录的末次冰期以来气候变化历史 [J]. 沉积学报, 29(6): 1170–1179. [Li C X, Song Y G, Qian L B, et al. 2011. History of climate change recorded by grain size at the Zhaosu loess section in the Central Asia since the Last Glacial period [J]. *Acta Sedimentologica Sinica*, 29(6): 1170–1179.]
- 李传想, 宋友桂, 王乐民. 2012. 新疆伊犁黄土元素地球化学特征及古环境意义 [J]. 新疆地质, 30(1): 103–108. [Li C X, Song Y G, Wang L M. 2012. Geochemical characteristics and Paleoenvironmental significance of the loess in the Ili region, Xinjiang [J]. *Xinjiang Geology*, 30 (1): 103–108.]
- 李传想, 宋友桂. 2011. 新疆伊犁黄土磁化率增强机制差异性分析 [J]. 地球学报, 32(1): 80–86. [Li C X, Song Y G. 2011. Differences in magnetic susceptibility enhancement in Ili Loess, Xinjiang [J]. *Acta Geoscientica Sinica*, 32(1): 80–86.]
- 李传想, 宋友桂. 2014. 西风区末次冰期以来昭苏黄土剖面微量元素分布特征及其环境意义 [J]. 地球环境学报, 5(2): 56–66. [Li C X, Song Y G. 2014. The characteristics of distribution of trace elements and their paleoclimatic implications at the Zhaosu Loess Section in Westerly Area since the Last Glacial Period [J]. *Journal of Earth Environment*, 5(2): 56–66.]
- 李珍, 张家武, 马海洲. 1999. 西宁黄土石英颗粒表面结构与黄土物质来源探讨 [J]. 沉积学报, 17(2): 221–225. [Li Z, Zhang J W, Ma H Z. 1999. Discession on the texture features of quartz grains and their origin in the Xining Loess [J]. *Acta Geographica Sinica*, 17(2): 221–225.]
- 李志忠, 凌智永, 陈秀玲, 等. 2010. 新疆伊犁河谷晚全新世风沙沉积粒度旋回与气候变化 [J]. 地理科学, 30(4): 613–619. [Li Z Z, Ling Z Y, Chen X L, et al. 2010. Late Holocene climate changes revealed by grain-size cycles in Takemukul desert in Yili of Xinjiang [J]. *Scientia Geographica Sinica*, 30(4): 613–619.]
- 刘东生. 1985. 黄土与环境 [M]. 北京: 科学出版社: 191–302. [Liu T S. 1985. Loess and the environment [M]. Beijing: Science Press: 191–302.]
- 潘仁义, 李川川, 张梅, 等. 2012. 天山冰川与塔克拉玛干风沙沉积的颗粒特征和分异过程分析 [J]. 北京大学学报(自然科学版), 48(5): 744–756. [Pan R Y, Li C C, Zhang M, et al. 2012. Analysis of particle characteristics and differentiation processes of glacial sediment in Tianshan and eolian sediment in the Taklimakan desert [J]. *Acta Scientiarum Naturalium Universitatis Pekinensis*, 48 (5): 744–756.]
- 石磊, 张跃, 陈艺鑫, 等. 2009. 贡嘎山海螺沟冰川沉积的石英砂扫描电镜形态特征分析 [J]. 北京大学学报(自然科学版), (2): 53–59. [Shi L, Zhang Y, Chen Y X, et al. 2009. Quartz grain SEM microtextures analysis of subglacial deposits at Hailuogou glacier [J]. *Acta Scientiarum Naturalium Universitatis Pekinensis (Online First)*, (2): 53–59.]
- 史正涛, 董铭, 方小敏. 2007. 伊犁盆地晚更新世黄土-古土壤磁化率特征 [J]. 兰州大学学报(自然科学版), 43(2): 7–10. [Shi Z T, Dong M, Fang X M. 2007. The characteristics of later pleistocene loess-paleosol magnetic susceptibility in Yili Basin [J]. *Journal of Lanzhou University (Natural Sciences)*, 43(2): 7–10.]
- 宋友桂, Nie Jun-sheng, 史正涛, 等. 2010b. 天山黄土磁化率增强机制初步研究 [J]. 地球环境学报, 1(1): 66–72. [Song Y G, Nie J S, Shi Z T, et al. 2010b. A preliminary study of magnetic enhancement mechanisms of the Tianshan Loess [J]. *Journal of Earth Environment*, 1(1): 66–72]
- 宋友桂, 史正涛, 方小敏, 等. 2010a. 伊犁黄土的磁学性质及其与黄土高原对比 [J]. 中国科学:D辑, 40(1): 61–72. [Song Y G, Shi Z T, Fang X M, et al. 2010a. Magnetic properties of the Ili loess and the comparison with Chinese Loess Plateau [J]. *Science China: Earth Sciences*, 40(1): 61–72.]
- 孙有斌. 2001. 黄土样中石英单矿物的分离 [J]. 岩矿测试, 20(1): 23–26. [Sun Y B. 2001. Separation of quartz minerals from loess samples [J]. *Rock and Mineral Analysis*, 20(1): 23–26.]
- 王颖, 迪纳瑞尔. 1985. 石英砂表面结构模式图集 [M]. 北京: 科学出版社: 4–30. [Wang Y, Deonarine B. 1985. Model atlas of surface textures of quartz sand [M]. Beijing: Science Press: 4–30.]
- 夏敦胜, 陈发虎, 马剑英, 等. 2010. 新疆伊犁地区典型黄土磁学特征及其环境意义初探 [J]. 第四纪研究, 30(5): 902–911. [Xia D S, Chen F H, Ma J Y, et al. 2010. Magnetic characteristics of loess in the Ili area and their environmental implication [J]. *Quaternary Sciences*, 30 (5): 902–911.]

- 夏训诚. 1987. 库木塔格沙漠的基本特征 [M]. 北京: 科学出版社: 78–94. [Xia X C. 1987. Essential characteristics of Kumtag desert [M]. Beijing: Science Press: 78–94.]
- 谢又予. 1984. 中国石英砂表表面结构特征图谱 [M]. 北京: 海洋出版社: 4–10. [Xie Y Y. 1984. Atlas of quartz sand surface textural features of China micrographs [M]. Beijing: Ocean Press: 4–10.]
- 杨晓平, 李 安, 黄伟亮. 2012. 天山北麓活动褶皱带晚第四纪时期隆升的差异性 [J]. 中国科学: 地球科学, 42(12): 1877–1888. [Yang X P, Li A, Huang W L. 2012. Differentiation in uplifting of active fold band located at the northern piedmonts of Tianshan mountains in the Late Quaternary [J]. *Science China: Earth Sciences*, 42(12): 1877–1888.]
- 叶 珮, 桑长青, 赵兴有. 2003. 新疆黄土分布规律及粉尘来源 [J]. 中国沙漠, 23(5): 514–520. [Ye W, Sang C Q, Zhao X Y. 2003. Spatial-temporal distribution of loess and source of dust in Xinjiang [J]. *Journal of Desert Research*, 23(5): 514–520.]
- 叶 珮. 2001. 新疆西风区黄土沉积特征与古气候 [M]. 北京: 海洋出版社: 1–180. [Ye W. 2001. Sedimental characteristics of loess in Westerly area, Xinjiang and paleoclimate [M]. Beijing: Ocean Press: 1–180.]
- 曾蒙秀, 宋友桂. 2014. 新疆伊犁地区近地表黄土的磁化率研究 [J]. 地球环境学报, 5(2): 135–144. [Zeng M X, Song Y G. 2014. Magnetic susceptibility characteristics of near-surface loess in the Ili basin, Xinjiang [J]. *Journal of Earth Environment*, 5(2): 135–144.]
- Amelinckx S. 1964. Solid state physics, Suppl. 6: The direct observation of dislocations [M]. New York: Academic Press: 1–53.
- Avouac J P, Tapponnier P, Bai M, et al. 1993. Active thrusting and folding along the northern Tien Shan and late Cenozoic rotation of the Tarim relative to Dzungaria and Kazakhstan [J]. *Journal of Geophysical Research: Solid Earth* (1978–2012), 98(B4): 6755–6804.
- Bull P A, Culver S J, Gardner R. 1980. Chattermark trails as paleoenvironmental indicators [J]. *Geology*, 8(7): 318–322.
- Bull P A. 1981. Environmental reconstruction by electron microscopy [J]. *Progress in Physical Geography*, 5(3): 368–397.
- Costa P J M, Andrade C, Mahaney W C, et al. 2013. Aeolian microtextures in silica spheres induced in a wind tunnel experiment: Comparison with aeolian quartz [J]. *Geomorphology*, 180: 120–129.
- Gallet S, Jahn B M, Lanoë B V V, et al. 1998. Loess geochemistry and its implications for particle origin and composition of the upper continental crust [J]. *Earth and Planetary Science Letters*, 156(3/4): 157–172.
- Guo Z T, Peng S Z, Hao Q Z, et al. 2001. Origin of the Miocene-Pliocene Red-Earth formation at Xifeng in northern China and implications for paleoenvironments [J]. *Palaeogeography, Palaeoclimatology, Palaeoecology*, 170 (1/2): 11–26.
- Guo Z T, Ruddiman W F, Hao Q Z, et al. 2002. Onset of Asian desertification by 22 Myr ago inferred from loess deposits in China [J]. *Nature*, 416(6877): 159–163.
- Holland P, Huang P H, Diffendal R F. 1997. SEM analysis of quartz sand grain surface textures indicates alluvial/colluvial origin of the Quaternary “glacial” boulder clays at Huangshan (Yellow Mountain), East-Central China [J]. *Quaternary Research*, 48(2): 177–186.
- Higgs R. 1979. Quartz-grain surface features of Mesozoic/Cenozoic sands from the Labrador and western Greenland continental margins [J]. *Journal of Sedimentary Research*, 49(2): 599–610.
- Kovacs J, Varga G, Dezso J. 2008. Comparative study on the Late Cenozoic red clay deposits from China and Central Europe (Hungary) [J]. *Geological Quarterly*, 52(4): 369–381.
- Krinsley D H, Donahue J. 1968. Environmental interpretation of sand grain surface textures by electron microscopy [J]. *Geological Society of America Bulletin*, 79(6): 743–748.
- Krinsley D, Cavallero L. 1970. Scanning electron microscopic examination of periglacial eolian sands from Long Island, New York [J]. *Journal of Sedimentary Research*, 40(4): 1345–1350.
- Krinsley D, Trusty P. 1985. Environmental interpretation of quartz grain surface textures [M]. Berlin: Springer: 213–229.
- Liu J F, Guo Z T, Qiao Y S, et al. 2006. Eolian origin of the Miocene loess-soil sequence at Qin'an, China: Evidence of quartz morphology and quartz grain-size [J]. *Chinese Science Bulletin*, 51(1): 117–120.
- Mahaney W C, Kalm V. 2000. Comparative scanning electron microscopy study of oriented till blocks, glacial grains and Devonian sands in Estonia and Latvia [J]. *Boreas*, 29(1): 35–51.
- Mahaney W C, Stewart A, Kalm V. 2001. Quantification of

- SEM microtextures useful in sedimentary environmental discrimination [J]. *Boreas*, 30(2): 165–171.
- Mahaney W C. 2002. Atlas of sand grain surface textures and applications [M]. New York: Oxford University Press: 237.
- Margolis S V, Krinsley D H. 1974. Processes of formation and environmental occurrence of microfeatures on detrital quartz grains [J]. *American Journal of Science*, 274(5): 449–464.
- Marzolf J E. 1976. Sand-grain frosting and quartz overgrowth examined by scanning electron microscopy: the Navajo Sandstone (Jurassic (?)), Utah [J]. *Journal of Sedimentary Research*, 46(4): 906–912.
- Moldvay L. 1962. On the governing sedimentation from eolian suspension [J]. *Acta Universitatis Szegediensis*, 14: 75–109.
- Nahon D, Trompette R. 1982. Origin of siltstones: glacial grinding versus weathering [J]. *Sedimentology*, 29(1): 25–35.
- Newsome D, Ladd P. 1999. The use of quartz grain microtextures in the study of the origin of sand terrains in Western Australia [J]. *Catena*, 35(1): 1–17.
- Peterknecht K M, Tietz G F. 2011. Chattermark trails: surface features on detrital quartz grains indicative of a tropical climate [J]. *Journal of Sedimentary Research*, 81(1/2): 153–158.
- Pittman E D. 1972. Diagenesis of quartz in sandstones as revealed by scanning electron microscopy [J]. *Journal of Sedimentary Research*, 42(3): 507–519.
- Porter J J. 1962. Electron microscopy of sand surface texture [J]. *Journal of Sedimentary Research*, 32(1): 124–135.
- Pye K, Sperling C. 1983. Experimental investigation of silt formation by static breakage processes: the effect of temperature, moisture and salt on quartz dune sand and granitic regolith [J]. *Sedimentology*, 30(1): 49–62.
- Pye K. 1983. Formation of quartz silt during humid tropical weathering of dune sands [J]. *Sedimentary Geology*, 34: 267–282.
- Pye K. 1987. Aeolian dust and dust deposits [M]. London: Academic Press: 1–165.
- Pye K. 1995. The nature, origin and accumulation of loess [J]. *Quaternary Science Reviews*, 14: 653–667.
- Schumm S, Stevens M. 1973. Abrasion in place: a mechanism for rounding and size reduction of coarse sediments in rivers [J]. *Geology*, 1(1): 37–40.
- Smalley I, O'Hara-Dhand K, Wint J, et al. 2009. Rivers and loess: The significance of long river transportation in the complex event-sequence approach to loess deposit formation [J]. *Quaternary International*, 198: 7–18.
- Smalley I. 1990. Possible formation mechanisms for the modal coarse-silt quartz particles in loess deposits [J]. *Quaternary International*, 7: 23–27.
- Smalley I. 1995. Making the material: the formation of silt-sized primary mineral particles for loess deposits [J]. *Quaternary Science Reviews*, 14: 645–651.
- Song Y G, Chen X L, Qian L B, et al. 2014. Distribution and composition of loess sediments in the Ili Basin, Central Asia [J]. *Quaternary International*, 334: 61–73.
- Song Y G, Lai Z P, Li Y, et al. 2015. Comparison between luminescence and radiocarbon dating of late Quaternary loess from the Ili Basin in Central Asia [J]. *Quaternary Geochronology*, 30: 405–410.
- Song Y G, Shi Z T, Dong H M, et al. 2008. Loess magnetic susceptibility in Central Asia and its paleoclimatic significance [C]// IEEE International Geoscience and Remote Sensing Symposium, Boston, MA, 7—11 July, 2008, 2: 1227–1230.
- Vos K, Vandenberghe N, Elsen J. 2014. Surface textural analysis of quartz grains by scanning electron microscopy (SEM): From sample preparation to environmental interpretation [J]. *Earth-Science Reviews*, 128: 93–104.
- Whalley W B, Marshall J R, Smith B J. 1982. Origin of desert loess from some experimental-observations [J]. *Nature*, 300(5891): 433–435.
- Wright J S. 2001. “Desert” loess versus “glacial” loess: quartz silt formation, source areas and sediment pathways in the formation of loess deposits [J]. *Geomorphology*, 36(3/4): 231–256.
- Wright J, Smith B, Whalley B. 1998. Mechanisms of loess-sized quartz silt production and their relative effectiveness: laboratory simulations [J]. *Geomorphology*, 23: 15–34.
- Xiao J L, Porter S C, An Z S, et al. 1995. Grain size of quartz as an indicator of winter monsoon strength on the Loess Plateau of central China during the last 130,000 yr [J]. *Quaternary Research*, 43(1): 22–29.
- Yang S L, Forman S L, Song Y G, et al. 2014. Evaluating OSL-SAR protocols for dating quartz grains from the loess in Ili Basin, Central Asia [J]. *Quaternary Geochronology*, 20: 78–88.
- Zhang W X, Shi Z T, Chen G J, et al. 2013. Geochemical characteristics and environmental significance of Taledé loess-paleosol sequences of Ili Basin in Central Asia [J]. *Environmental Earth Sciences*, 70(5): 2191–2202.